Supplementary Information

Supplementary Information Figure 1: Pathways of collagen cross-linking following lysyl oxidase oxidation of collagen

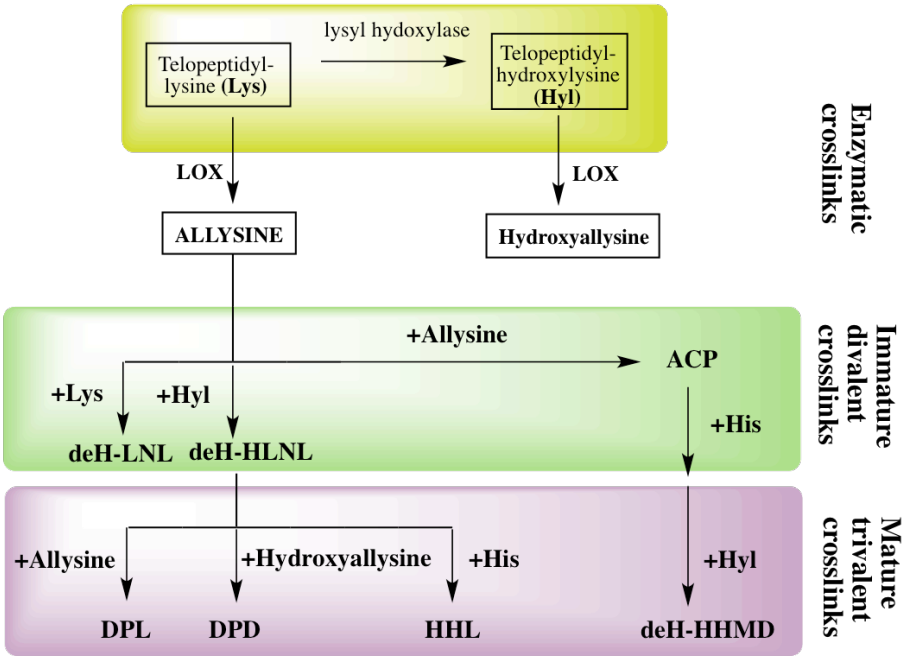

deH-LNL: dehydro-lysinonorleucine, **deH-HLNL**: dehydro-hydroxylysinonorleucine, **ACP**: aldol condensation product, **HHL**: histidinohydroxylysininorleucine, **deH-HHMD**: dehydro-histidinohydroxymerodesmosine, **DPL**: Deoxypyrrolodine, **DPD**: Deoxypyridinoline.

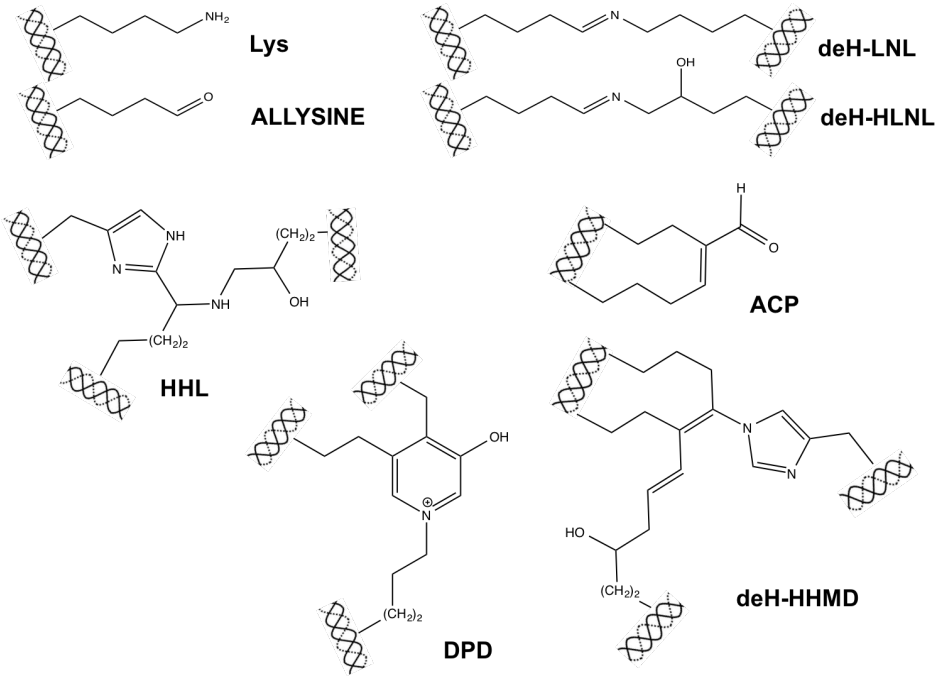

Fig. S1: Top panel: pathways of collagen cross-linking after LOX oxidation of collagen lysines. Bottom panel: structures of immature and mature collagen crosslinks

Supplementary Information Figure 2: Stability of GdOA

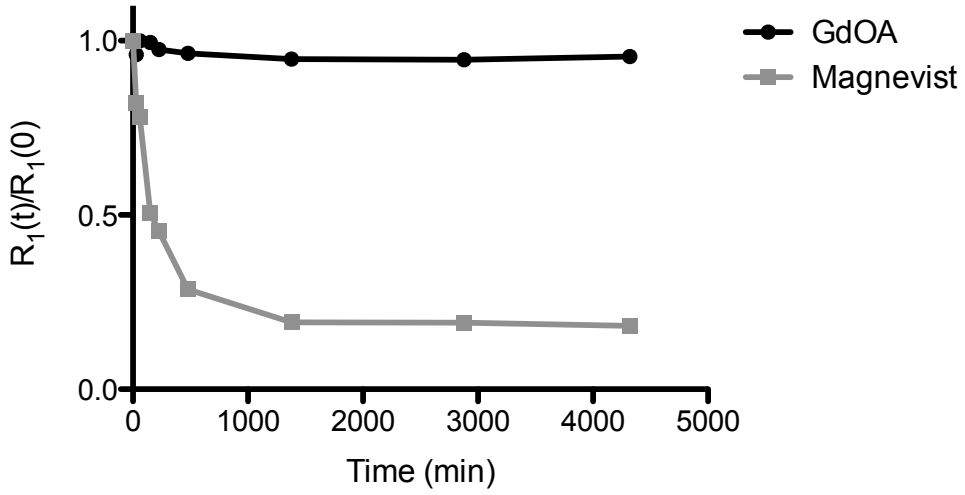

Fig. S2: Evolution of the relative water proton paramagnetic longitudinal relaxation rate $R_1(t)/R_1(0)$ vs. time for GdOA and Magnevist (Gd-DTPA) when challenged with Zn^{2+} and phosphate at pH 7, 37 °C. A decrease in $R_1(t)/R_1(0)$ is indicative of Gd^{3+} release from the complex and precipitation as the insoluble phosphate salt. Transmetallation of GdDTPA under these conditions is consistent with literature. There is no evidence of transmetallation for the DOTA-based, macrocyclic GdOA complex, in keeping with the high kinetic inertness and thermodynamic stability of macrocyclic gadolinium chelates.

Supplementary Information Figure 3: Blood half-lives in bleomycin-treated mice imaged with GdOA and GdOX confirms similar pharmacokinetics of GdOA and GdOX.

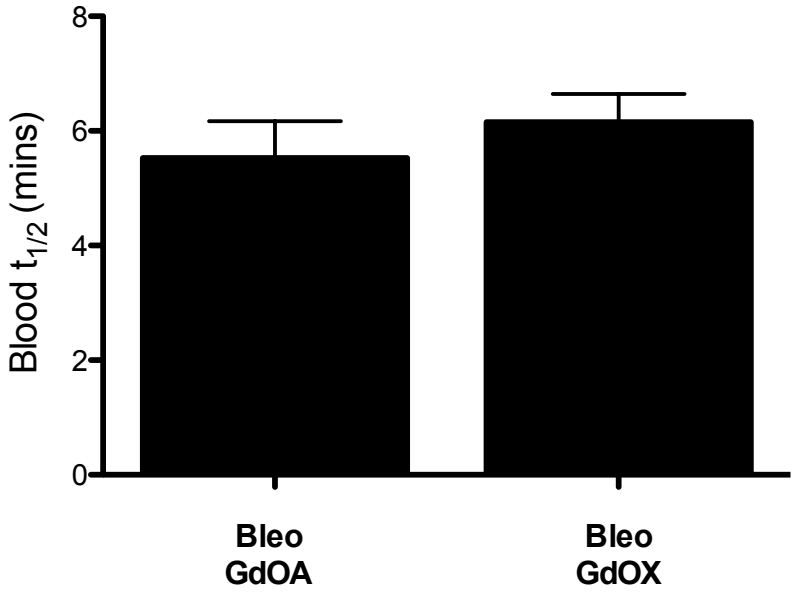

Fig. S3: Blood half-lives of GdOA and GdOX in mice as determined from dynamic MRI are similar in bleomyocin-challenged mice.

Supplementary Information Figure 4: Histology slides graded for pulmonary fibrosis by Ashcroft scoring show increased fibrotic burden in bleomycin treated animals compared to naïve cohort

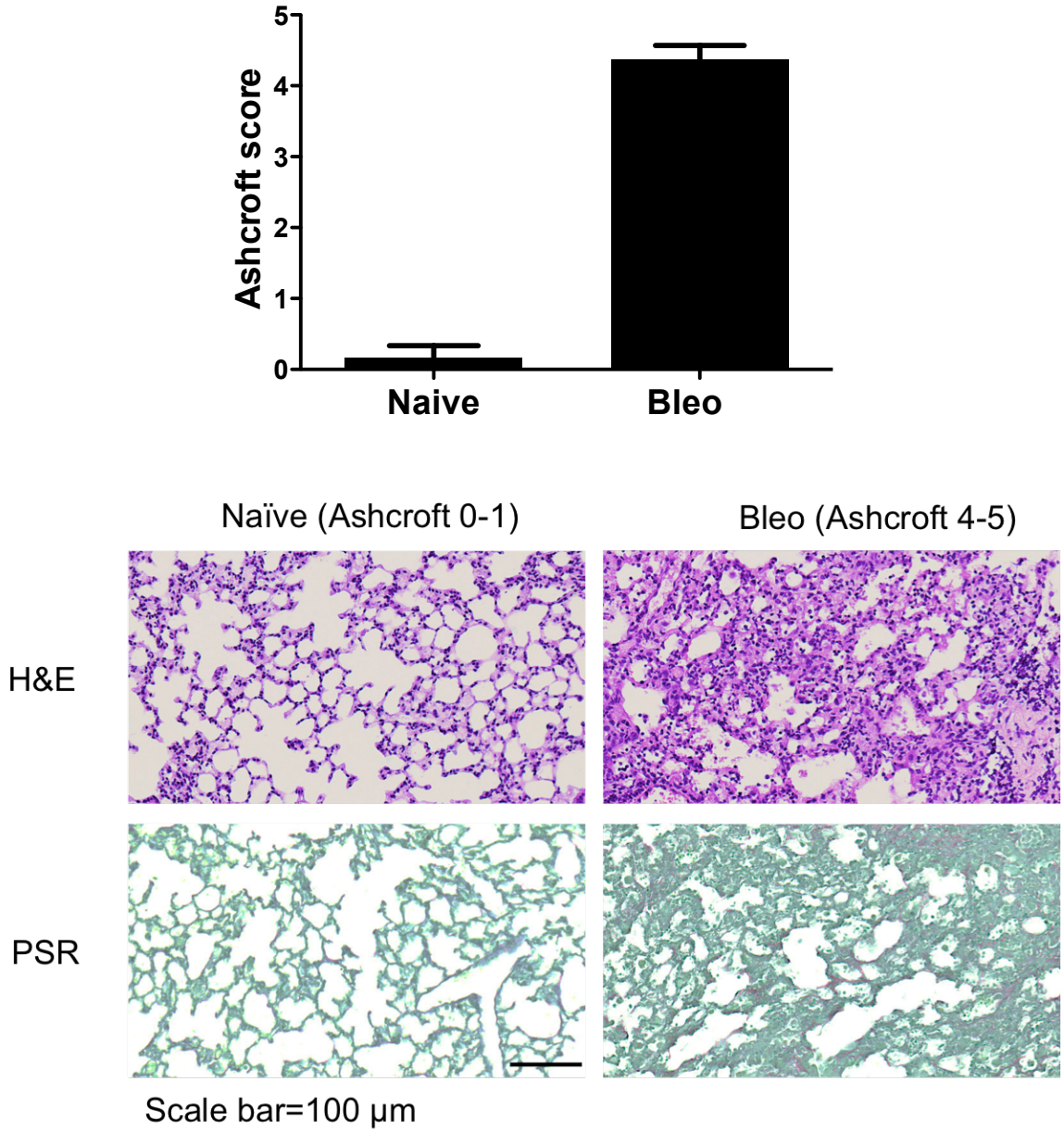

Fig. S4: Hematoxylin and Eosin (H&E) stained lung tissue and Pico Sirius Red (PSR) stained lung tissue was assessed by a pulmonary pathologist and scored for lung injury according to the Ashcroft scoring system. The bleomycin treated mice had significant lung injury whereas the lungs of naïve mice were unaffected.

Supplementary Information Figure 5: Total lysyl oxidase (LOX) enzyme activity in naive, bleomycin-treated, bleomycin+daily BAPN-treated mice and bleomycin+daily PBS-treated mice imaged with GdOA and GdOX confirms LOX activity elevation in bleomycin treated mice. A significant decrease in LOX activity is seen when BAPN is administered and LOX activity blocked.

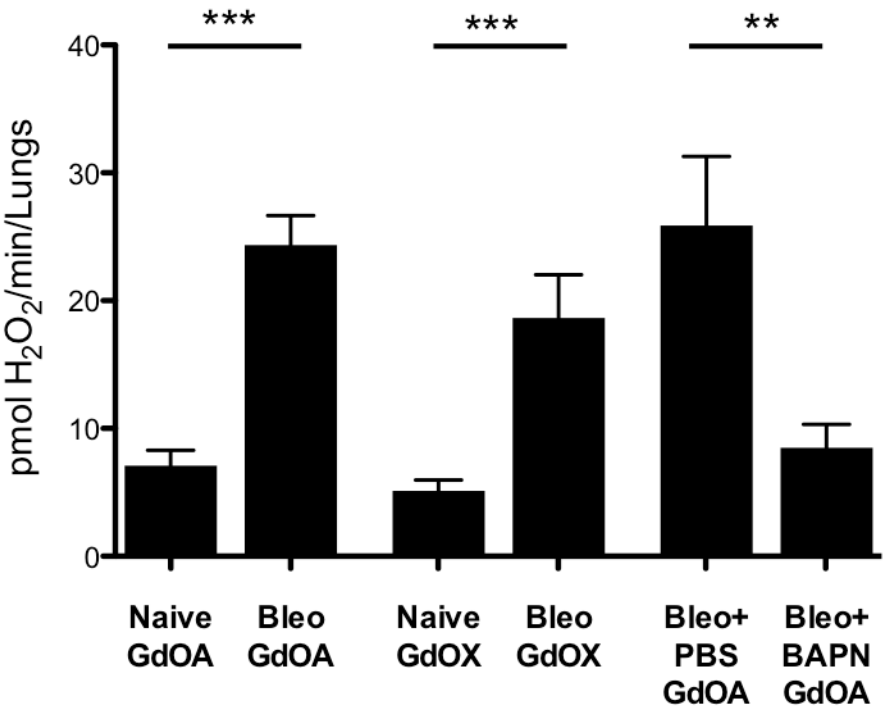

Fig. S5: Total LOX enzyme activity in in Naïve, Bleomycin and Bleomycin+BAPN lung treatment groups (**: P<0.01, ***: P< 0.001).

Supplementary Information Figure 6: Hydroxyproline concentration in naive, bleomycin-treated, bleomycin+daily BAPN-treated mice and bleomycin+daily PBS-treated mice imaged with GdOA and GdOX confirms increase in collagen accumulation in mice treated with bleomycin

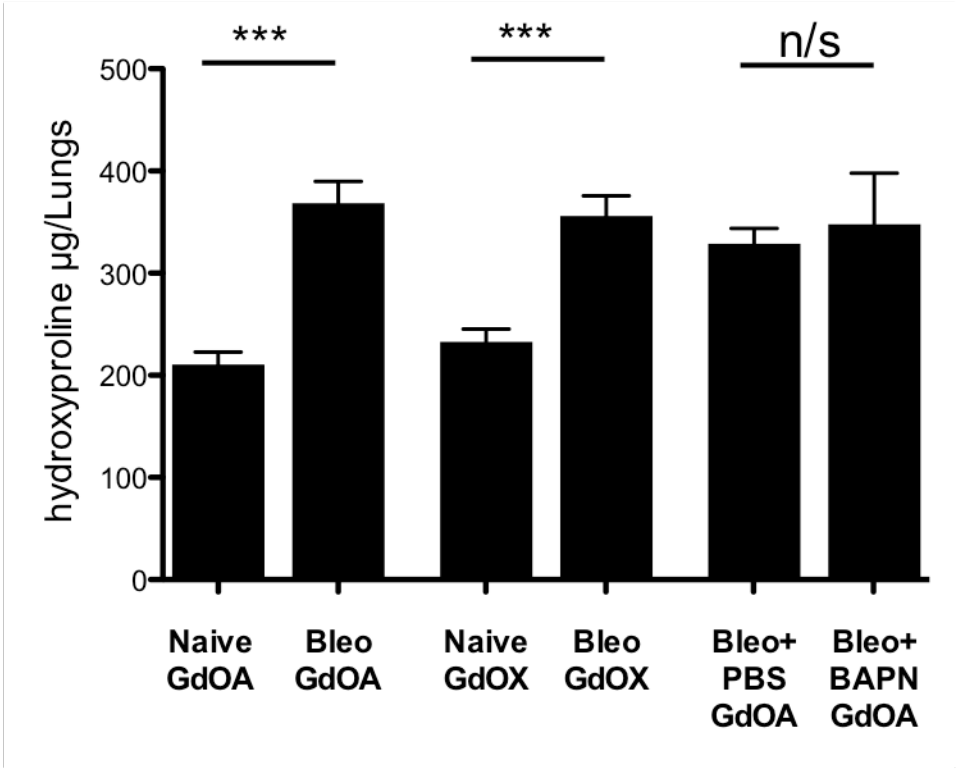

Fig. S6: Hydroxyproline lung concentrations in Naïve, Bleomycin and Bleomycin+BAPN lung treatment groups (*:P < 0.05, **: P<0.01, ***: P< 0.001, n/s: not significant).

Supplementary Information Figure 7: Allysine concentration in naive, bleomycin-treated, bleomycin+daily BAPN-treated mice and bleomycin+daily PBS-treated mice imaged with GdOA and GdOX confirms allysine elevation in bleomycin treated mice. A significant decrease in allysine is seen when BAPN is administered and LOX activity blocked.

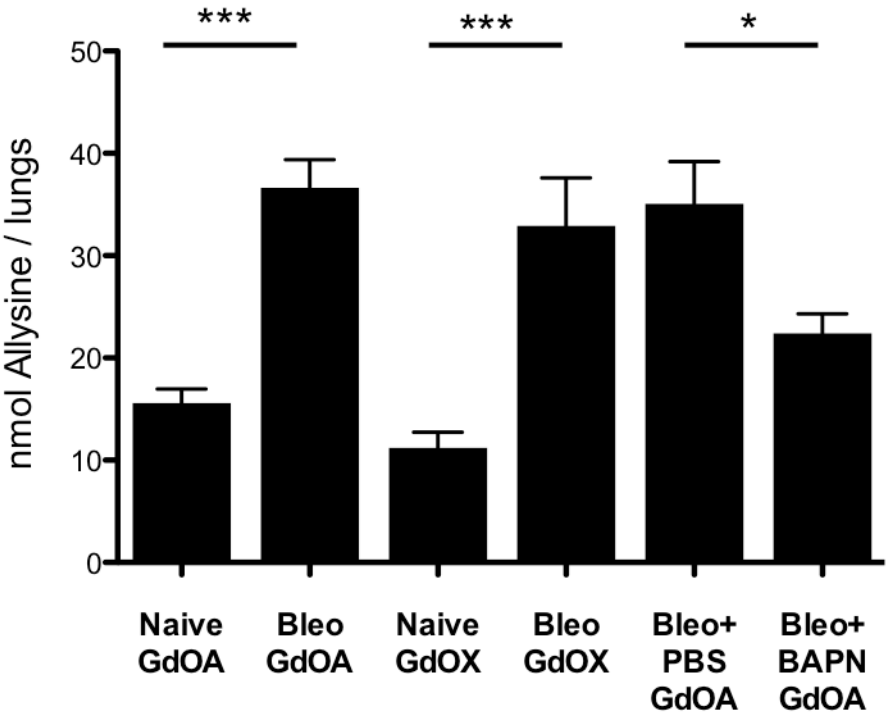

Fig. S7: Allysine concentrations in in Naïve, Bleomycin and Bleomycin+BAPN lung treatment groups (*:P < 0.05, ***: P< 0.001).

Supplementary Information Figure 8: Pre- and Post- UTE sequences

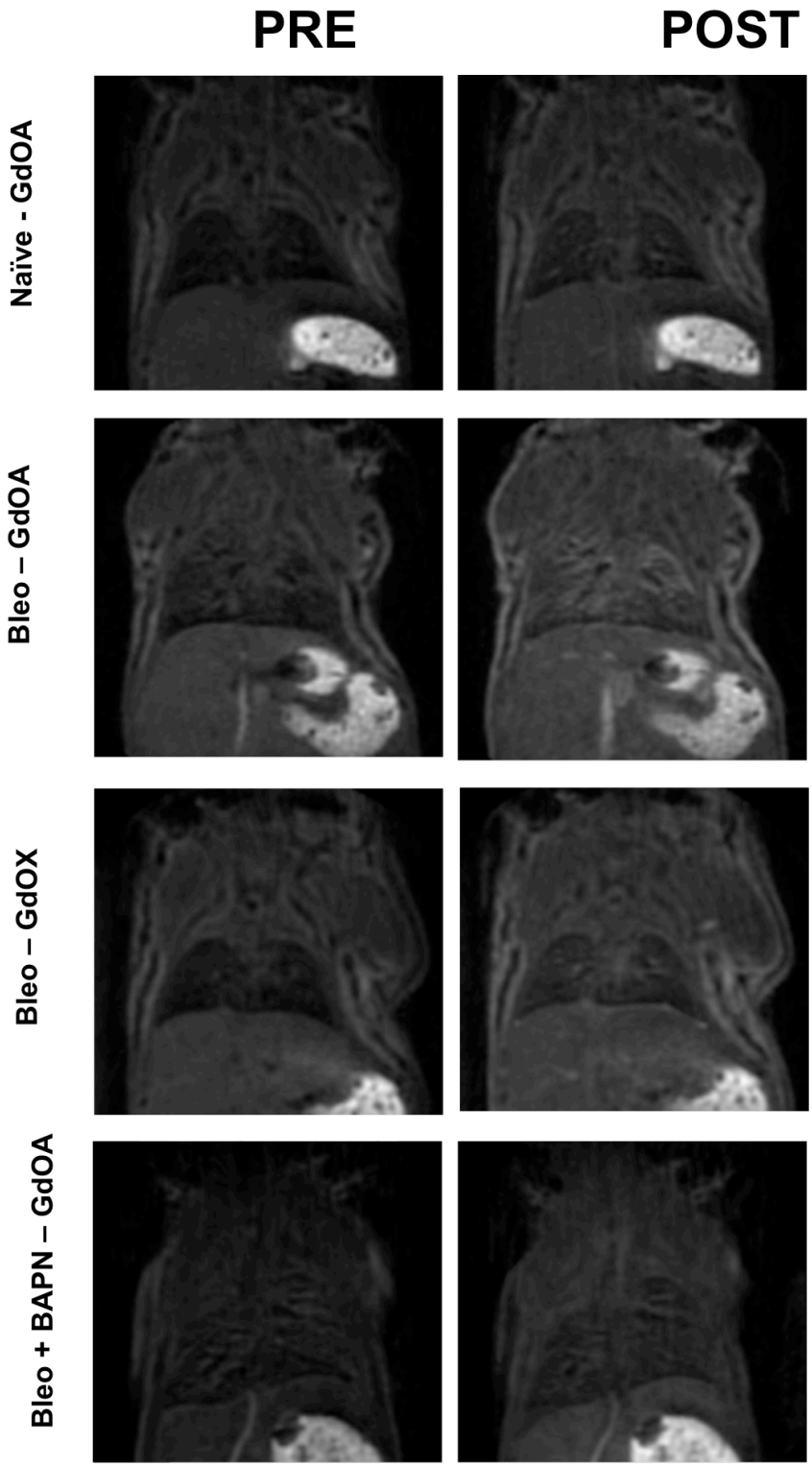

Fig S8: Pre- and Post- UTE sequences of GdOA in Naïve mice, GdOA in Bleomycin treated mice, GdOX in Bleomycin treated mice and GdOA in Bleomycin + BAPN treated mice

Supplementary Information Figure 9: MRI quantification of the change in lung-to-muscle signal ratio (ΔLMR) of naive, bleomycin-treated, bleomycin+daily BAPN-treated mice and bleomycin+daily PBS-treated mice imaged with GdOA and GdOX confirms disease specific GdOA signal enhancement in fibrotic lung.

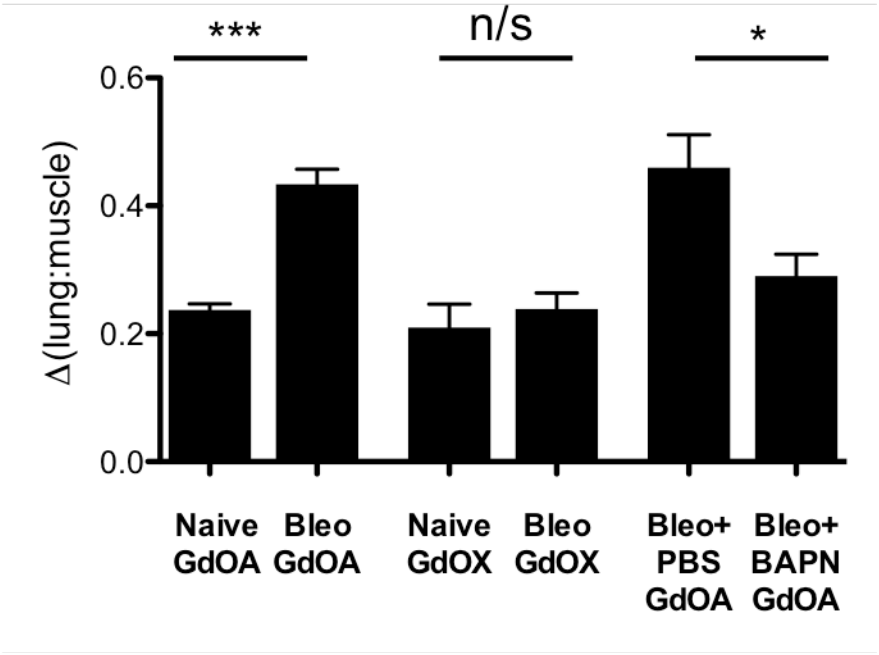

Fig. S9: ΔLMR quantification of GdOA and GdOX imaging of lung fibrosis (*:P < 0.05, ***: P< 0.001, n/s: not significant).

Supplementary Information Figure 10: Correlation between Δ(Lung:Muscle) signal ratio and allysine content and hydroxyproline content

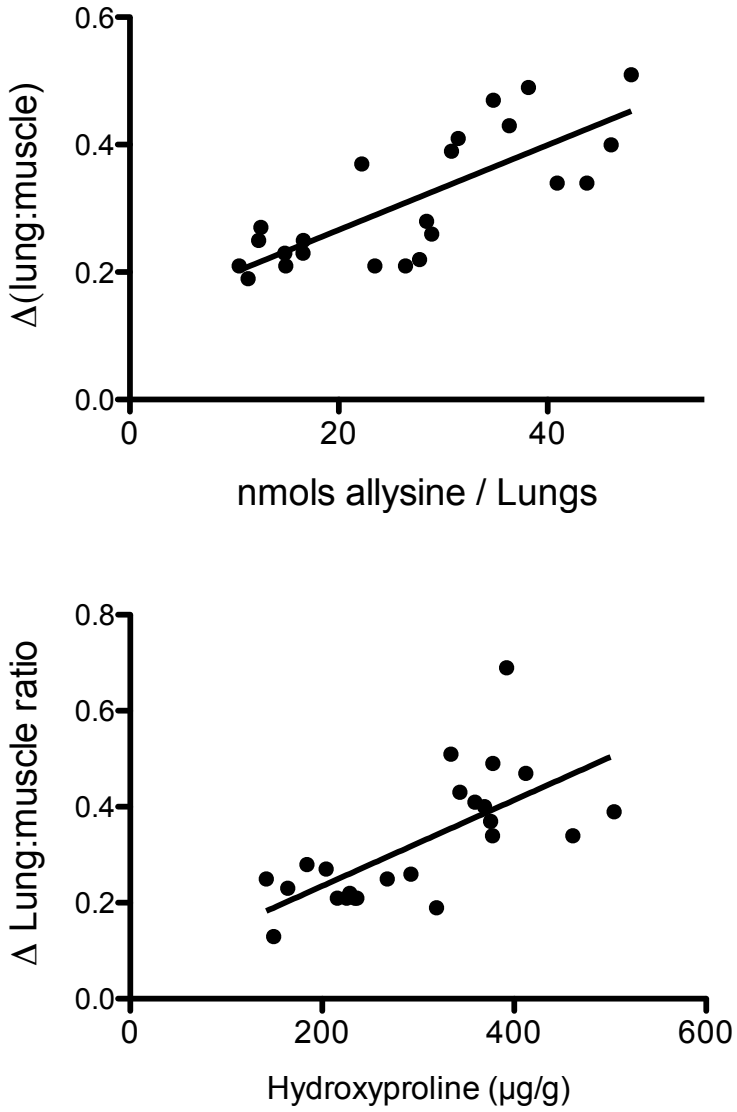

Fig. S10: The signal enhancement in bleomycin-treated and sham-treated mice imaged with GdOA correlates well with (TOP) allysine content (r = 0.77) and (BOTTOM) hydroxyproline content in tissue (r = 0.68).

Supplementary Information Figure 11: No significant difference in the Δ(liver-to-muscle) ratios for GdOA in naive and bleomycin treated mice indicates no non specific off-target probe accumulation in the liver.

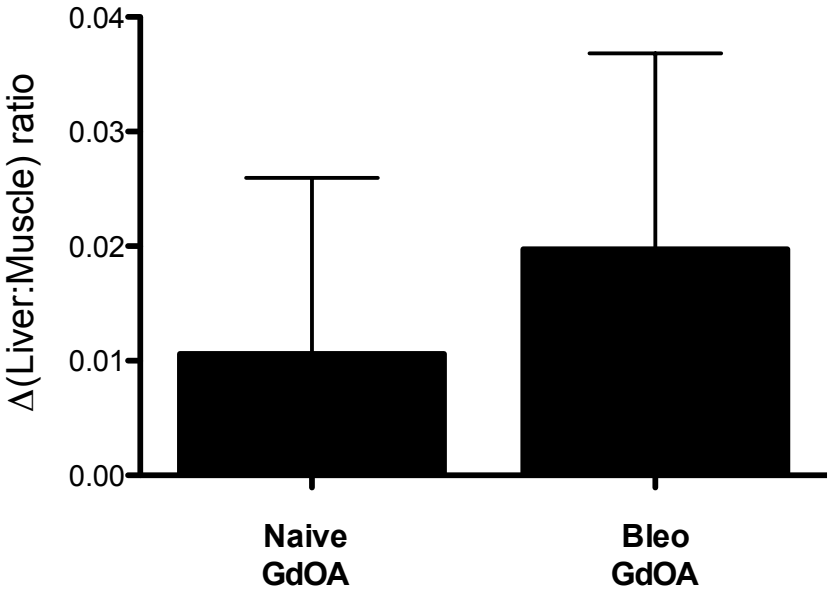

Fig S11: Δ(liver-to-muscle) ratio for GdOA in naïve and bleomycin treated mice

Supplementary Information Figure 12: Total Gd concentration as measured by ICP-MS analysis in naive, bleomycin-treated, bleomycin+daily BAPN-treated mice and bleomycin+daily PBS-treated mice imaged with GdOA and GdOX confirms increase in Gd uptake for GdOA in bleomycin treated mice. Lung uptake of GdOX in bleomycin treated mice and GdOA lung uptake in bleomycin treated mice when BAPN was co-administered remains at the same level as the uptake in naïve mice.

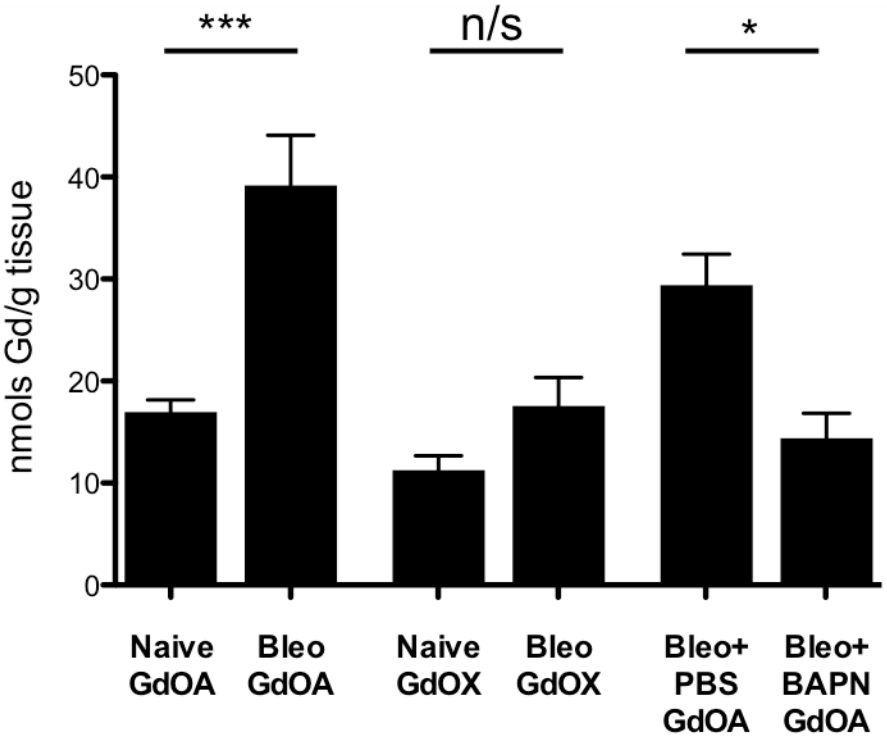

Fig. S12: Total Gd concentration in in Naïve, Bleomycin and Bleomycin+BAPN lung treatment groups (*:P < 0.05, ***: P< 0.001, n/s: not significant).

Organ	%ID per Gram	%ID per Organ
Serum	0.54±0.23	0.59±0.13
Lung	1.05±0.27	0.08±0.09
Liver	0.31±0.11	0.37±0.11
Muscle	0.27±0.10	1.86±0.39
Heart	0.56±0.69	0.03±0.01
Spleen	0.36±0.08	0.07±0.02
Intestine	0.44±0.27	0.79±0.06
Stomach	0.48±0.15	0.07±0.02
Bone	0.23±0.11	0.05±0.01
Kidneys	3.94±1.28	1.06±0.13
Tail	3.53±3.62	N/A

Supplemental Table 1: Gd-OA is readily cleared from the body. Biodistribution of Gd-OA at 1 hours after bolus intravenous injection in C57Bl/6 mice showed that 95% had already been eliminated from the body. The mean ± 1 standard deviation for each organ is tabulated. ID=Injected Dose.

Probe syntheses:

General methods:
All reactants and reagents were of commercial grade and were used without further purification.

NMR
NMR spectra were recorded on a Varian 500 NMR system equipped with a 5 mm broadband probe (^{1}H NMR: 499.81 MHz, ^{13}C: 125.68 MHz).

Preparative HPLC
Purifications were performed using the following methods:

Method 1:
Column: MetaChem Technologies Inc., LUNA C18(2) 10 μm 250×21.2 mm, UV detection at 220, and 254 nm, flow rate: 15 mL/min, solvent A: 0.1% TFA in water, solvent B: 0.1% TFA in MeCN, gradient: 0-2 mins hold at 5% B, 2-24 mins gradient to 95% B, 24-25 mins hold at 95% B, 25-28 mins gradient to 5% B, 28-30 mins re-equilibrate at 5% B.

Method 2:
Column: Restek, UltraAqueous C18, 5 μm 250×10 mm, UV detection at 220 nm, flow rate: 3 mL/min, solvent A: 0.1% TFA in water, B: 0.1% TFA in MeCN, gradient conditions: 0-5 mins hold at 2% B, 5-15 mins gradient to 20% B, 15-18 mins gradient to 60% B, 18-20 mins hold at 60% B, 20-22.5 mins gradient to 2% B, 22.5-25 mins re-equilibrate at 2% B.

HPLC-MS
HPLC-MS purity analysis was carried out on an Agilent 1260 system coupled to an Agilent Technologies 6130 Quadrupole MS system using the following methods:

Method A:
Column: Phenomenex Luna, C18(2), 100×2 mm, flow rate: 0.8 mL/min, UV detection at 220, 254 and 280 nm, solvent A: 0.1% formic acid in water, B: 0.1% formic acid in MeCN, gradient conditions: 0-1 mins hold at 5% B, 1-9 mins gradient to 95% B, 9-10 mins hold at 95% B, 10-12 mins gradient to 5% B, 12-15 mins re-equilibrate at 5% B.

Method B:
Column: Restek, UltraAqueous C18, 5 μm 250×4.6 mm, UV detection at 220 nm, flow rate: 0.8 mL/min, solvent A: 0.1% formic acid in water, B: 0.1% formic acid in MeCN, gradient conditions: 0-2 mins hold at 5% B, 2-12 mins gradient to 50% B, 12-13 mins gradient to 95% B, 13-15 mins hold at 95% B, 15-16 mins gradient to 5% B, 16-18 mins re-equilibrate at 5% B.

HPLC-ICP-MS
HPLC-ICP-MS purity analysis was carried out on an Agilent 1260 HPLC system coupled to an Agilent 8800-QQQ ICP-MS system, using the following HPLC method:
Column: Restek, UltraAqueous C18, 5 μm 250×4.6 mm, UV detection at 220 nm, flow rate: 0.8 mL/min, solvent A: 0.1% TFA in water, B: 0.1% TFA in MeCN, gradient conditions: 0-2 mins hold at 5% B, 2-12 mins gradient to 50% B, 12-13 mins gradient to 95% B, 13-15 mins hold at 95% B, 15-16 mins gradient to 5% B, 16-18 mins reequilibrate at 5% B.

UV Titration

Into a 1.5 mL quartz cuvette is placed 10 µL of ligand solution and 1 mL of an arsenazo III solution (10 µM arsenazo III in 0.15 M NH_4OAc buffer pH 7). The cuvette is placed into a UV/Vis spectrophotometer and zeroed at 656 nm. Aliquots of 10 µL of a 4.85 mM $Pb(NO_3)_2$ solution (or 0.485 mM solution close to the end point), are titrated into the cuvette until a positive absorbance is observed. A positive absorbance represents the end point of the titration.

Preparation of GdOA: 2,2',2''-(10-(5-(2-(aminooxy)acetamido)-1-carboxypentyl)-1,4,7,10-tetraazacyclododecane-1,4,7-triyl)triacetic acid gadolinium complex

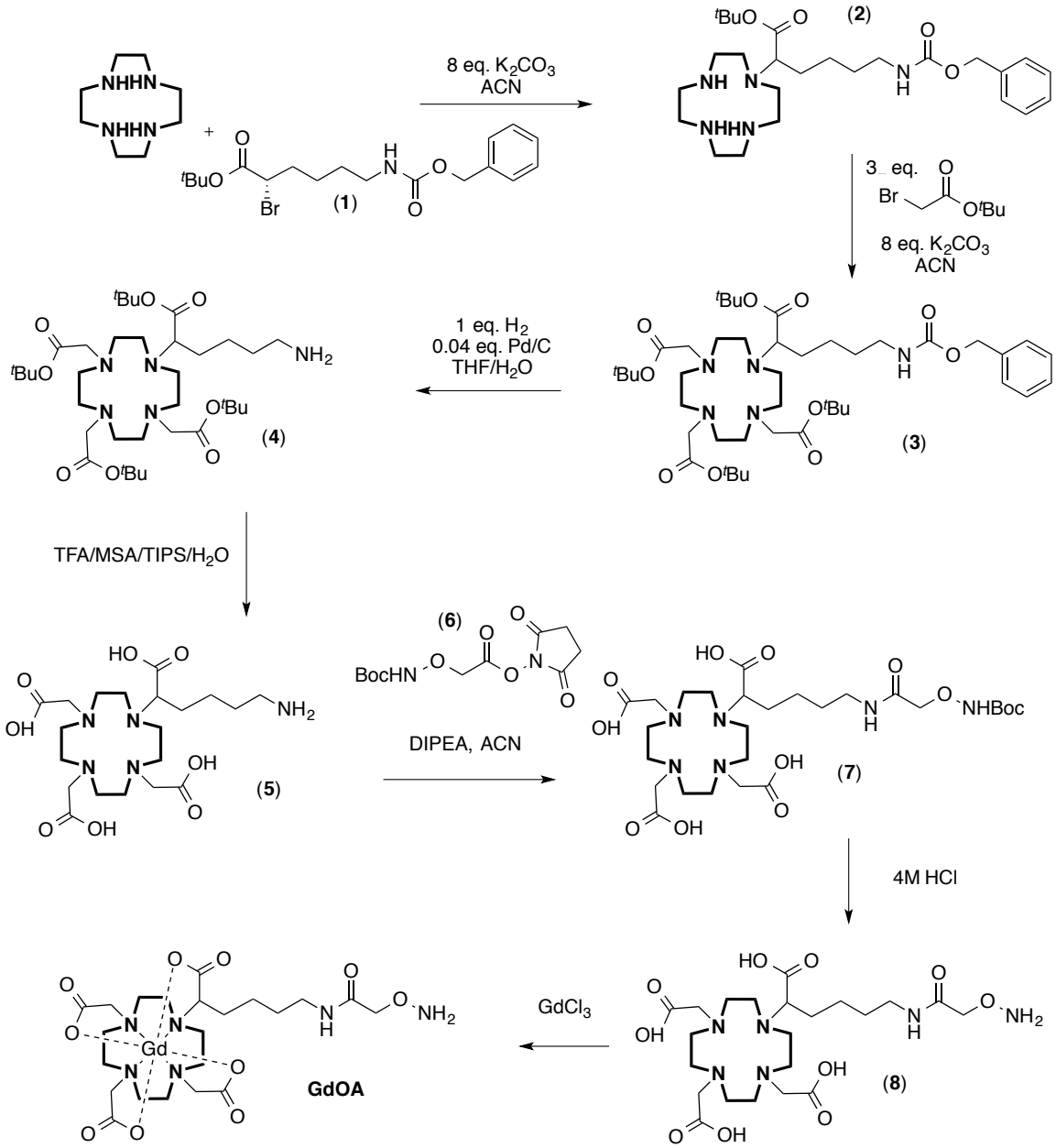

Scheme 1: Synthesis of GdOA from tetraazacyclododecane

Compounds *tert*-butyl 6-(((benzyloxy)carbonyl)amino)-2-bromohexanoate (**1**) and 2,5-dioxopyrrolidin-1-yl 2-(((*tert*-butoxycarbonyl)amino)oxy)acetate (**6**) were prepared according to literature protocols.[1]

tert-Butyl-6-(((benzyloxy)carbonyl)amino)-2-(1,4,7,10-tetraazacyclododecan-1-yl)hexanoate (2)

Tetraazacyclododecane (0.842 g, 4.89 mmol) and triethylamine (1.136 mL, 8.13 mmol) were dissolved in acetonitrile (25 mL). To this solution was added *tert*-butyl 6-(((benzyloxy)carbonyl)amino)-2-bromohexanoate (**1**) (0.650 g, 1.63 mmol) and the starting material consumption followed over time by LC/MS. After 6 h the solvent was evaporated and the residue purified by preparative HPLC (Method 1) to yield 0.731 g (1.49 mmol, 91%) of white solid product.

^{1}H ($CDCl_3$, 500 MHz, 25 °C): δ = 7.96 (br.s, 2H, NH), 7.28 (m, 5H, CH_2*Ph*), 5.37 (br.s, 1H, CON*H*), 5.06 (s, 2H, C*H*$_2$Ph), 3.28-2.88 (m, 19H, cyclen, C*H*$CO_2{}^t$Bu, C*H*$_2$NHCO), 1.56-1.41 (m, 15H, CHC*H*$_2$C*H*$_2$C*H*$_2$CH$_2$NHCO, CHC$O_2{}^t$*Bu*).

^{13}C ($CDCl_3$, 125 MHz, 25 °C): δ = 172.1, 156.7, 136.7, 128.5, 128.0, 127.6, 83.0, 66.4, 63.2, 47.0, 44.6, 43.3, 42.4, 40.4, 29.3, 28.4, 27.9, 24.1.

LC/MS (ESI+): $C_{26}H_{45}N_5O_4$: m/z calcd 492.35 [MH+]; found 492.4 (MH+)

tri-_tert_-Butyl 2,2',2''-(10-(6-(((benzyloxy)carbonyl)amino)-1-(_tert_-butoxy)-1-oxohexan-2-yl)-1,4,7,10-tetraazacyclododecane-1,4,7-triyl)triacetate (3)

tert-Butyl-6-(((benzyloxy)carbonyl)amino)-2-(1,4,7,10-tetraazacyclododecan-1-yl)hexanoate (**2**) (0.955 g, 1.94 mmol) and potassium carbonate (2.685 g, 19.4 mmol) were dissolved in dry acetonitrile (20 mL). *tert*-Butyl-2-bromoacetate (1.100 g, 5.64 mmol) dissolved in dry acetonitrile (40 mL) was added dropwise with starting material consumption followed by LC/MS over time. After 6h the solvent was evaporated and the residue purified by preparative HPLC (Method 1) to yield 1.491 g (0.179 mmol, 92%) of white solid product.

^{1}H ($NCCD_3$, 500 MHz, 50 °C): δ = 10.21 (br.s, 2H, N*H*), 7.34 (m, 5H, CH_2*Ph*), 5.64 (br.s, 1H, CON*H*), 5.05 (s, 2H, C*H*$_2$Ph), 3.89-3.00 (m, 25H, cyclen, 3xC*H*$_2CO_2{}^t$Bu, C*H*$CO_2{}^t$Bu, C*H*$_2$NHCO), 1.80-1.36 (m, 42H, CHC*H*$_2$C*H*$_2$C*H*$_2$CH$_2$NHCO, 4x$CO_2{}^t$*Bu*).

^{13}C ($NCCD_3$, 125 MHz, 50 °C): δ = 172.0, 170.5, 168.7, 157.7, 138.8, 129.6, 129.0, 128.7, 84.9, 84.0, 83.8, 66.9, 63.6, 56.0, 52.6 (2 C's), 50.6, 47.5, 41.5, 30.7, 28.7, 28.6, 28.5, 28.1, 25.3.

LC/MS (ESI+): $C_{44}H_{75}N_5O_{10}$: m/z calcd 834.56 [MH+]; found 834.4 (MH+)

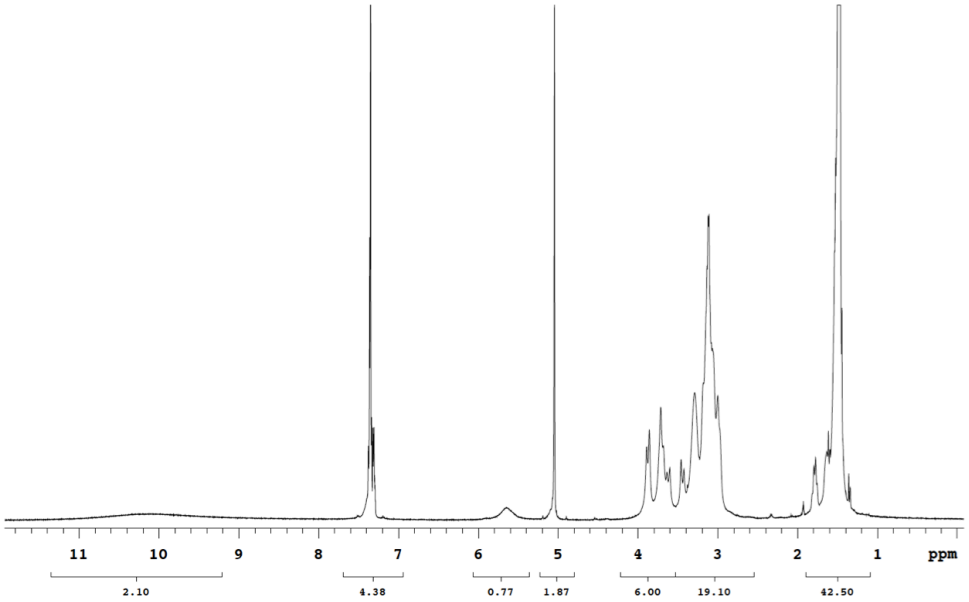

Fig. S12: ^{1}H NMR of (**3**)

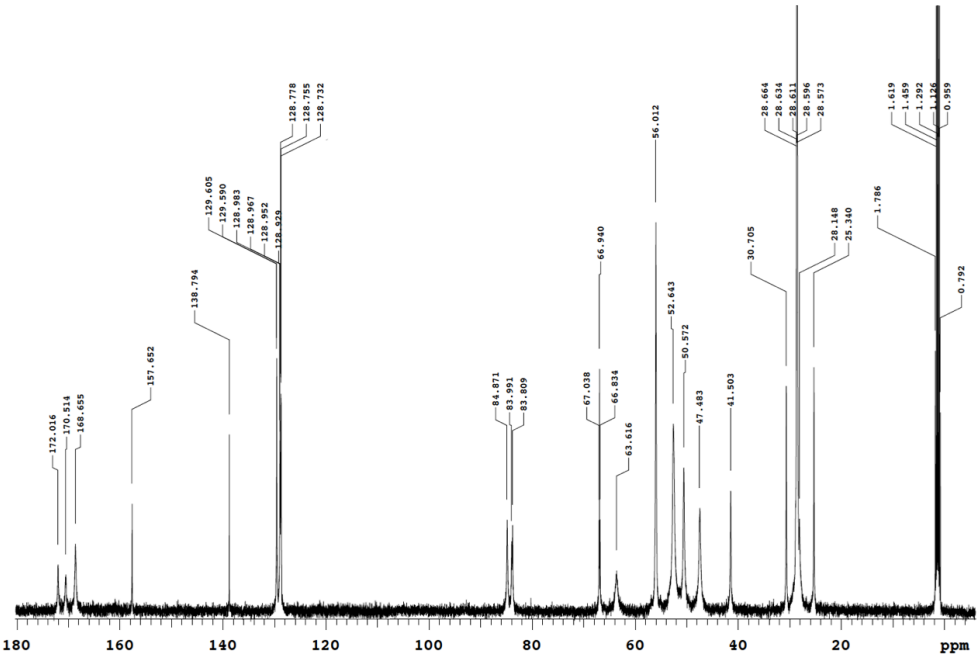

Fig. S13: ^{13}C NMR of (**3**)

tri-*tert*-Butyl 2,2',2''-(10-(6-amino-1-(*tert*-butoxy)-1-oxohexan-2-yl)-1,4,7,10-tetraazacyclododecane-1,4,7-triyl)triacetate (4)

tri-*tert*-Butyl 2,2',2''-(10-(6-(((benzyloxy)carbonyl)amino)-1-(*tert*-butoxy)-1-oxohexan-2-yl)-1,4,7,10-tetraazacyclododecane-1,4,7-triyl)triacetate (**3**) (1.200 g, 1.44 mmol) was added to a slurry of palladium on carbon (dry, 61.3 mg, 10% by mass) in anhydrous methanol (15 mL). The mixture was subject to two cycles of vacuum and hydrogen purge and then stirred under an atmosphere of hydrogen for 12 h. After evacuating the system of hydrogen, celite was added and the slurry filtered through a MeOH-wet bed of celite. The filtrate was concentrated in vacuo to a light yellow oil to yield 0.896 g (1.28 mmol, 89%) of product which was used in the next step without further purification.

^{1}H ($NCCD_3$, 500 MHz, 50 °C): δ = 9.34 (br.s, 3H, N*H*), 8.23 (br.s, 2H, N*H*), 3.86-2.98 (m, 25H, cyclen, 3x$CH_2CO_2{}^t$Bu, $CHCO_2{}^t$Bu, CH_2NHCO), 1.83-1.37 (m, 42H, $CHCH_2CH_2CH_2CH_2$NHCO, 4x$CO_2{}^tBu$).

^{13}C ($NCCD_3$, 125 MHz, 50 °C): δ = 172.9, 171.5, 169.6, 84.8, 84.1, 83.8, 65.2, 57.3, 56.6, 53.8, 51.2, 48.4, 44.1, 41.0, 29.5, 29.3, 28.8, 28.5, 27.3, 25.7.

LC/MS (ESI+): $C_{36}H_{69}N_5O_8$: m/z calcd 700.52 [MH+]; found 700.7 (MH+)

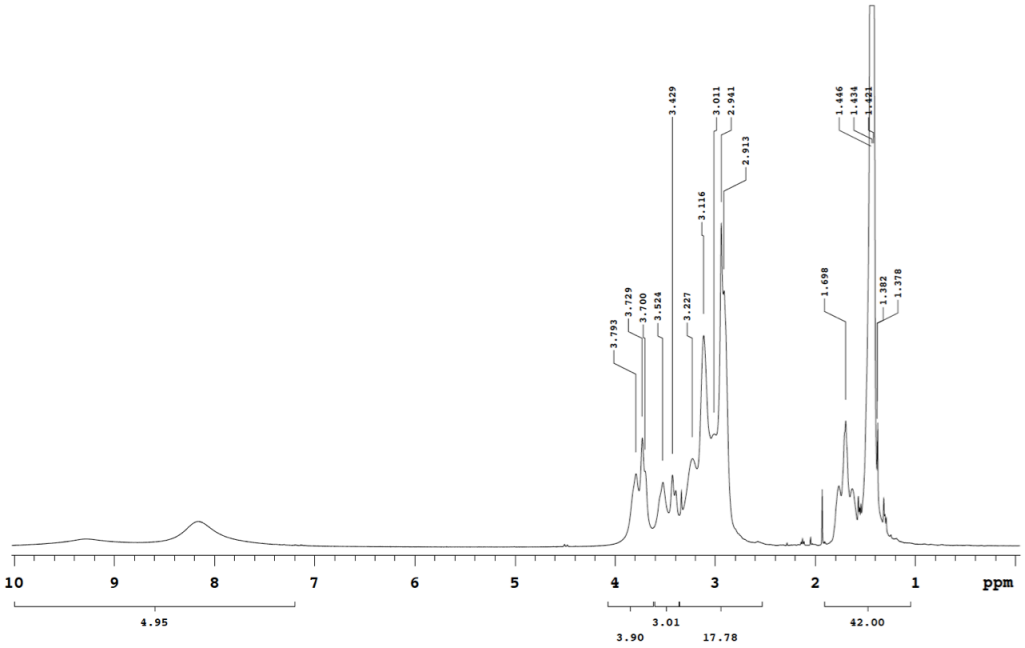

Fig. S14: ^{1}H NMR of (**4**)

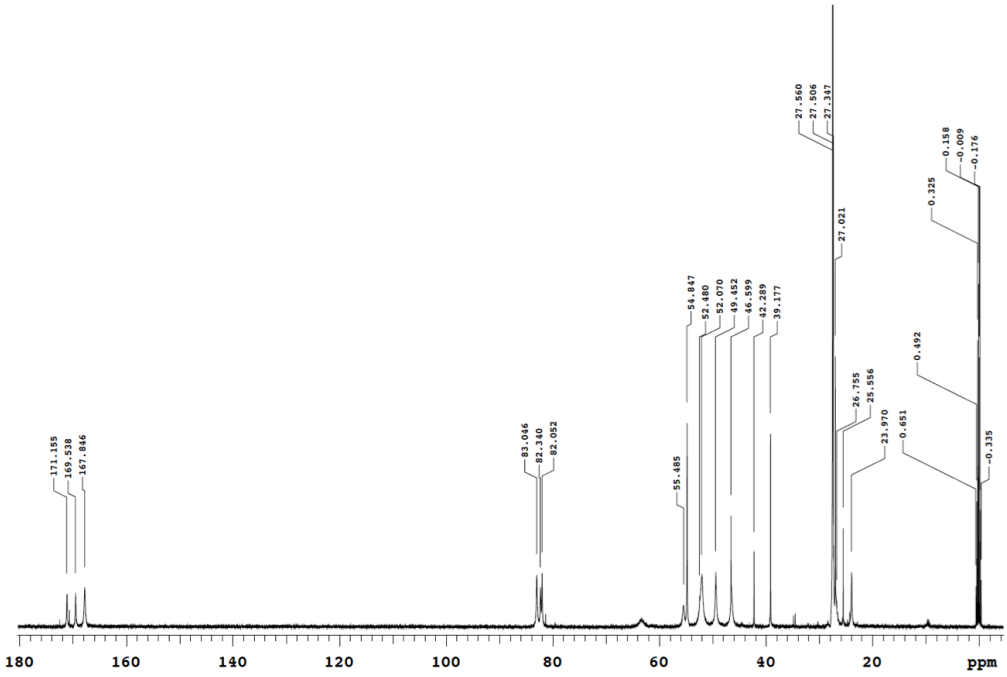

Fig. S15: ^{13}C NMR of (**4**)

2,2',2''-(10-(5-Amino-1-carboxypentyl)-1,4,7,10-tetraazacyclododecane-1,4,7-triyl)triacetic acid (5)

tri-*tert*-Butyl 2,2',2''-(10-(6-amino-1-(*tert*-butoxy)-1-oxohexan-2-yl)-1,4,7,10-tetraazacyclododecane-1,4,7-triyl)triacetate (**4**) (0.896 g, 1.28 mmol) was dissolved in a mixture of TFA (15 mL), triisopropyl silane (900 µL) and water (900 µL) and the mixture was stirred at room temperature overnight. The volatiles were removed in vacuo and a white solid precipitated with diethyl ether 0.572 g (1.20 mmol, 94%), which was used in the next step without further purification.

^{1}H (d_6-DMSO, 500 MHz, 60 °C): δ = 10.10 (br. s, 5H, CO_2H, N*H*), 7.95 (s, 3H, NH_3^+), 3.84 (m, 4H, CH_2CO_2H), 3.63 (m, 3H, $CHCO_2H$, CH_2CO_2H), 3.05-2.80 (m, 18H, cyclen + CH_2NH_2), 1.7-1.44 (m, 6H, $CHCH_2CH_2CH_2CH_2NH_2$).

^{13}C (d_6-DMSO, 125 MHz, 60 °C): δ = 172.8, 171.7, 169.2, 61.4, 54.5, 53.8, 51.1, 50.9, 48.8, 46.1, 38.4, 27.3, 26.6, 23.3.

LC/MS (ESI+): $C_{20}H_{37}N_5O_8$: m/z calcd 476.27 [MH+]; found 476.5 (MH+)

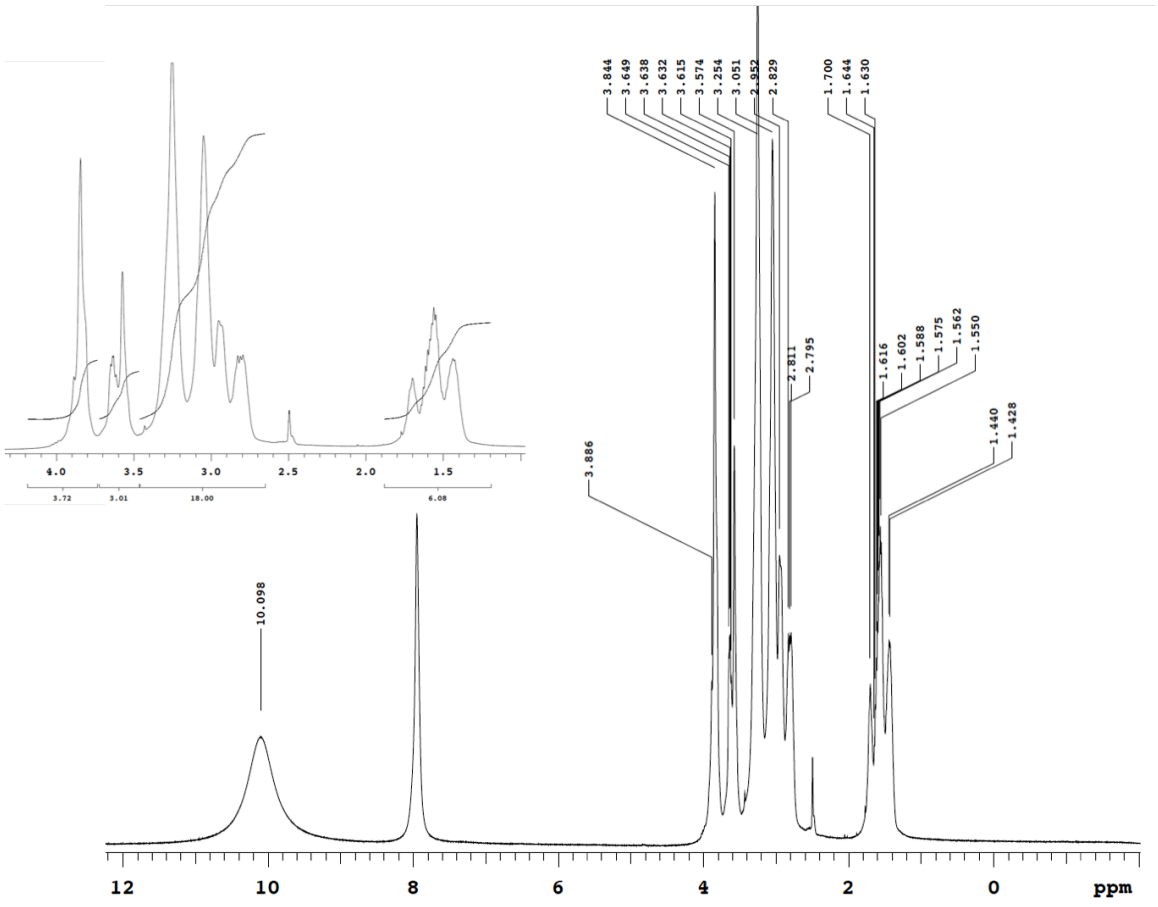

Fig. S16: ^{1}H NMR of (**5**)

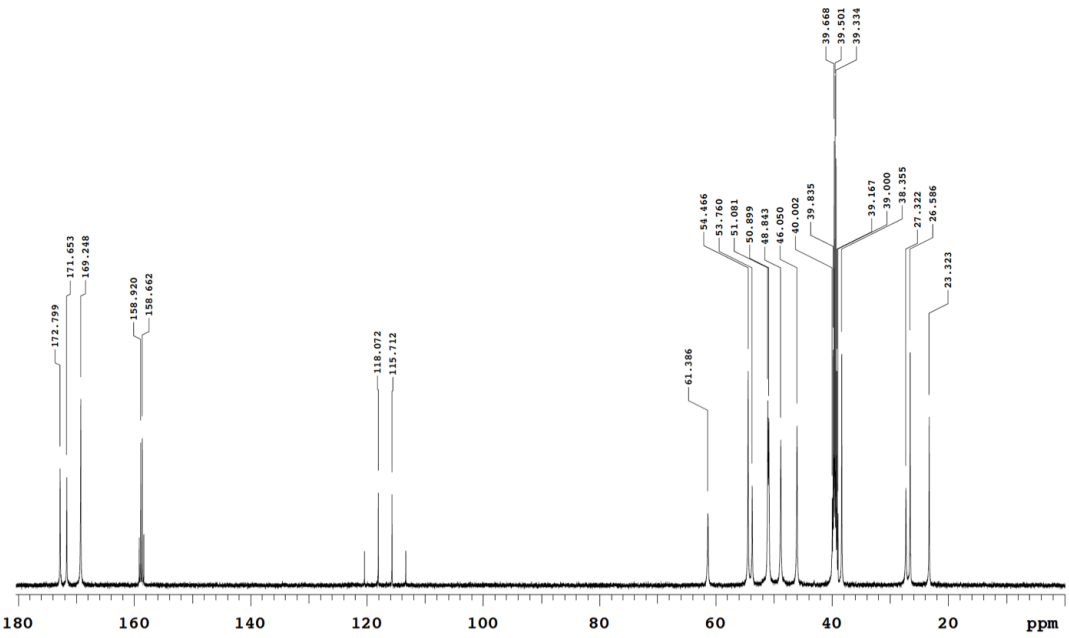

Fig. S17: ^{13}C NMR of (**5**)

2,2',2''-(10-(14-Carboxy-2,2-dimethyl-4,8-dioxo-3,6-dioxa-5,9-diazatetradecan-14-yl)-1,4,7,10-tetraazacyclododecane-1,4,7-triyl)triacetic acid (7)

2,2',2''-(10-(5-Amino-1-carboxypentyl)-1,4,7,10-tetraazacyclododecane-1,4,7-triyl)triacetic acid (**5**) (0.572 g, 1.20 mmol) and diisopropylethylamine (1.05 mL, 1.26 mmol) were dissolved in dry DMF (10 mL). After 5 min 2,5-dioxopyrrolidin-1-yl 2-(((*tert*-butoxycarbonyl)amino)oxy)acetate (**6**) (0.416 g, 1.44 mmol) was added and stirring continued for 24 h. The solvent was evaporated and the residue purified by preparative HPLC (Method 3) to yield 0.652 g (1.00 mmol, 84%) of white solid product.

^{1}H (d_6-DMSO, 500 MHz, 70 °C): δ = 4.14 (s, 2H, CH_2ONH$_2$), 3.43-3.00 (m, 25H, cyclen, 3xCH_2CO$_2$H, CHCO$_2$H, CH_2NHCO), 1.68-1.38 (m, 15H, CHCH_2CH_2CH_2CH$_2$NHCO, CO$_2$^{t}*Bu*).

^{13}C (d_6-DMSO, 125 MHz, 70 °C): δ = 171.6, 170.5, 167.6, 164.0, 156.5, 80.1, 74.6, 64.1, 55.4, 51.2, 49.6, 47.5, 37.9, 28.7, 27.8, 24.2, 20.9, 19.2, 18.8.

LC/MS (ESI+): $C_{27}H_{48}N_6O_{12}$: m/z calcd 649.34 [MH+]; found 649.6 (MH+)

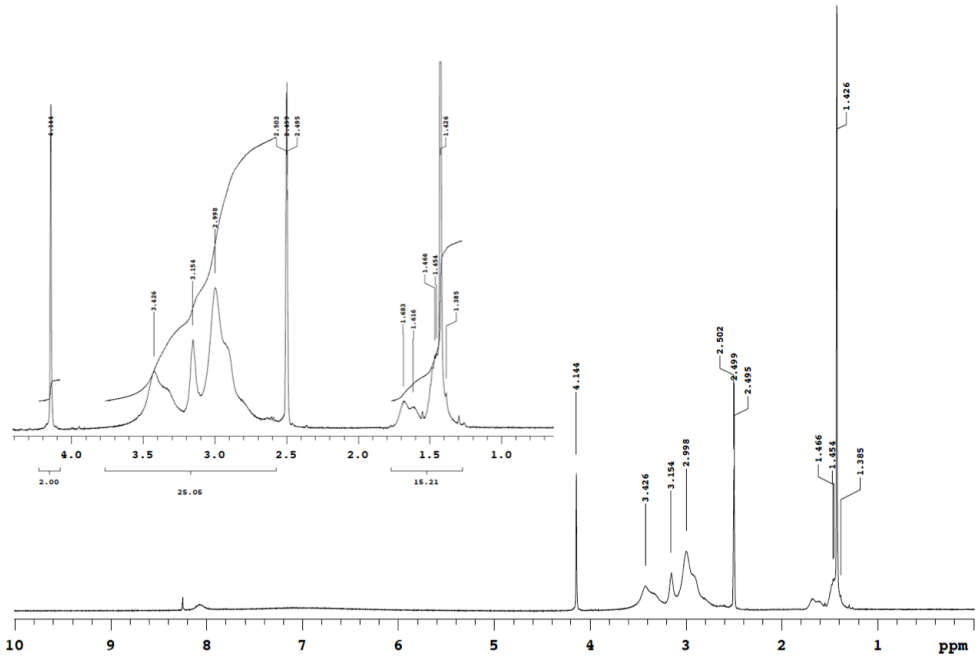

Fig. S18: ^{1}H NMR of (**7**)

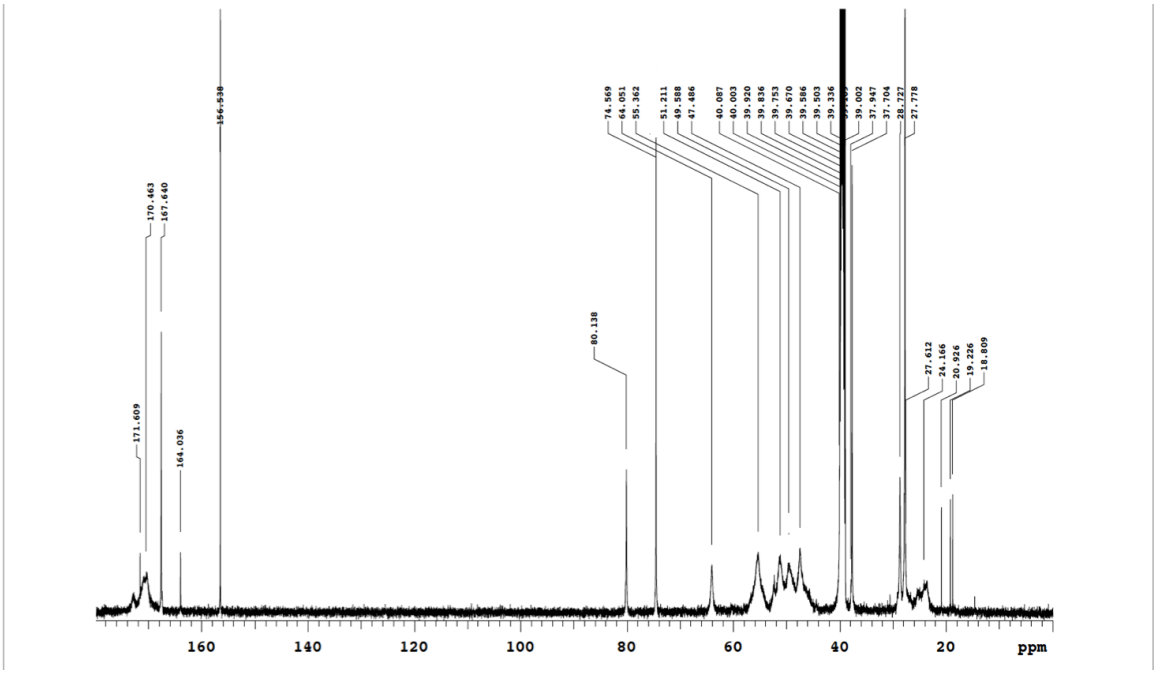

Fig. S19: ^{13}C NMR of (**7**)

2,2',2''-(10-(5-(2-(aminooxy)acetamido)-1-carboxypentyl)-1,4,7,10-tetraazacyclododecane-1,4,7-triyl)triacetic acid (8)

2,2',2''-(10-(14-carboxy-2,2-dimethyl-4,8-dioxo-3,6-dioxa-5,9-diazatetradecan-14-yl)-1,4,7,10-tetraazacyclododecane-1,4,7-triyl)triacetic acid (**7**) (0.250 g, 0.39 mmol) was dissolved in 4 M HCl in dioxane (4 mL) and stirred at room temperature overnight. The volatiles were removed in vacuo. The residue was redissolved in water and the pH adjusted to 7 using ammonium hydroxide. After lyophilisation the solid was redissolved in water and subjected to a UV titration using arsenazo III to determine the concentration of ligand (0.200 g, 0.36 mmol, 95%).

^{1}H (D_2O, 500 MHz, 50 °C): δ = 5.13 (s, 2H, CH_2ONH$_2$), 4.56-4.51 (m, 5H, 2xCH_2CO$_2$H, CHCO$_2$H), 4.36 (s, 2H, CH_2CO$_2$H), 4.11-3.84 (m, 18H, cyclen, CONHCH_2), 2.40 (m, 2H, CHCH_2), 2.24 (m, 2H, CHCH$_2$CH$_2$CH_2), 2.15 (m, 2H, CHCH$_2$CH_2CH$_2$).

^{13}C (D_2O, 125 MHz, 50 °C, CD_3OD spike): δ = 174.8, 173.5, 170.7, 169.9, 73.1, 61.8, 56.0, 54.3 51.5, 50.7, 49.3, 46.1, 39.1, 28.5, 28.0, 24.0.

LC/MS (ESI+): $C_{22}H_{40}N_6O_{10}$: m/z calcd 549.29 [MH+]; found 549.4 (MH+)

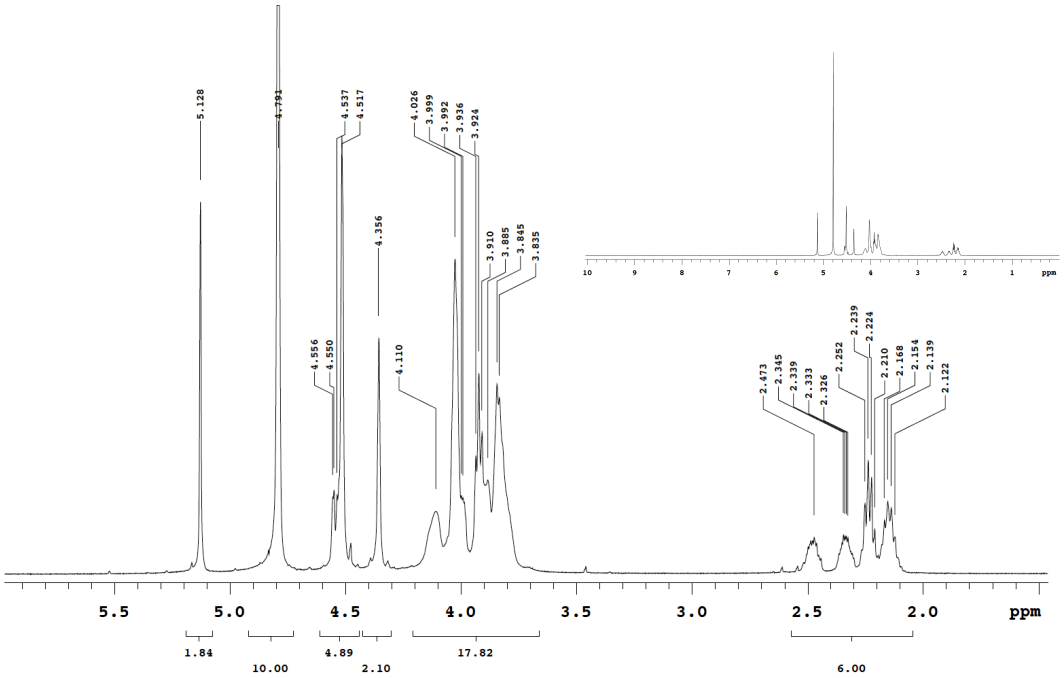

Fig. S20: ^{1}H NMR of (**8**)

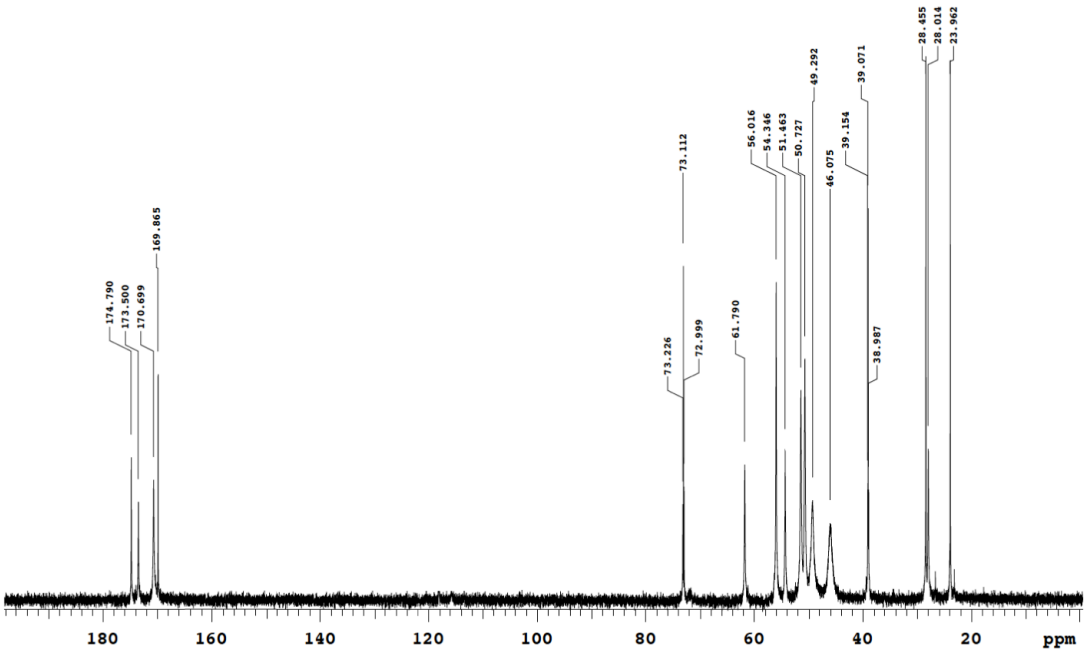

Fig. S21:-^{13}C NMR of (**8**)

2,2',2''-(10-(5-(2-(aminooxy)acetamido)-1-carboxypentyl)-1,4,7,10-tetraazacyclododecane-1,4,7-triyl)triacetic acid gadolinium complex (**GdOA**)

The stock solution of 2,2',2''-(10-(5-(2-(aminooxy)acetamido)-1-carboxypentyl)-1,4,7,10-tetraazacyclododecane-1,4,7-triyl)triacetic acid (0.10 g, 0.18 mmol) was treated with $GdCl_3.6H_2O$ (0.071 g, 0.19 mmol) and the pH adjusted to 6.2. After 12 h of stirring at r.t., the pH was adjusted to 5.5 and the solution passed through a chelex column. The pH was adjusted to 7.0 and the solution lyophilized to yield a white solid (0.12 g, 0.17 mmol, 94%).
LC/MS (ESI+): $C_{22}H_{36}GdN_6O_{10}$: m/z calcd 703.17 [MH+]; found 703.1 (MH+)

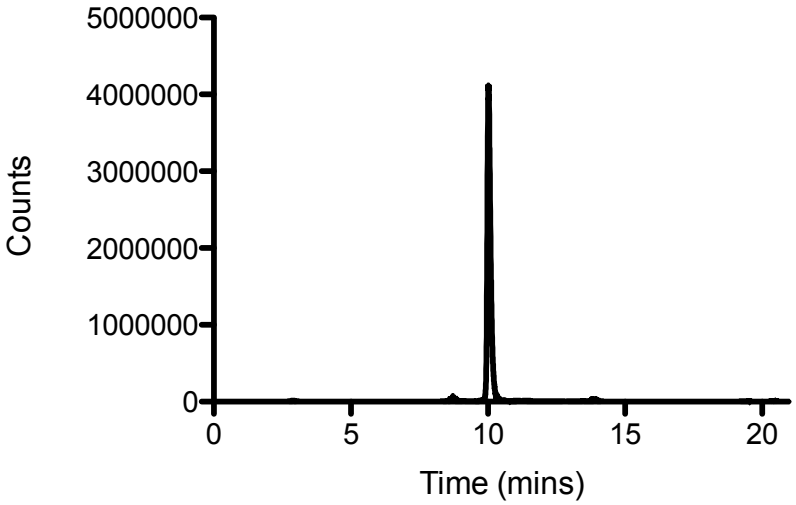

Fig. S22: HPLC with ICP-MS detection of Gd for the GdOA sample.

Preparation of GdOX: 2,2',2''-(10-(5-(2-(methoxy)acetamido)-1-carboxypentyl)-1,4,7,10-tetraazacyclododecane-1,4,7-triyl)triacetic acid gadolinium complex

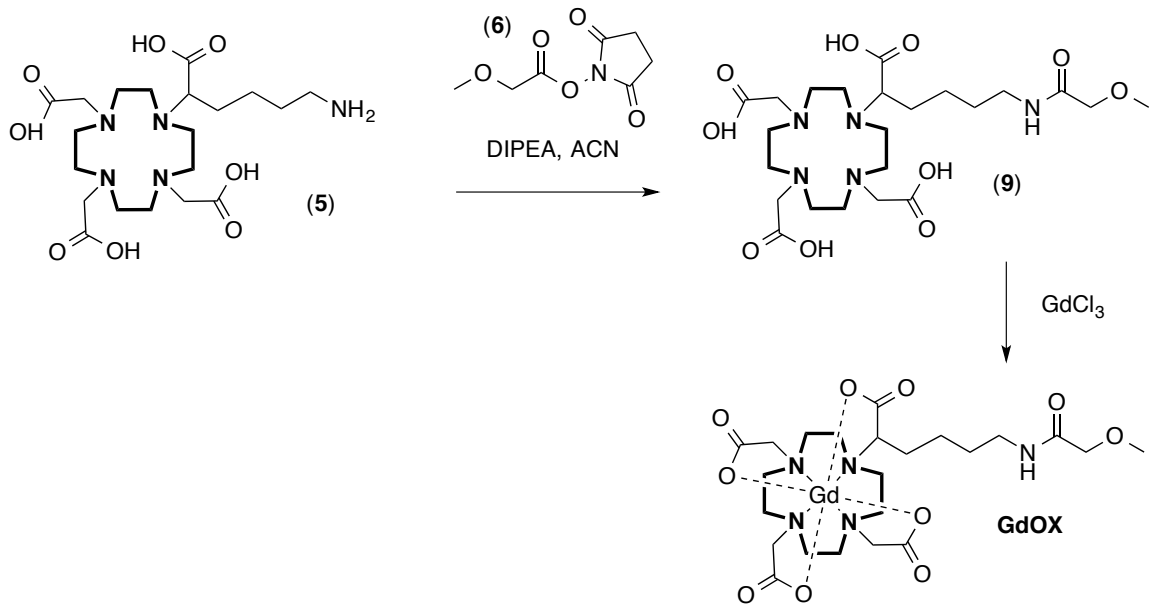

Scheme 2: Synthesis of Gd-OX from DOTA-NH_2(5)

(**6**) was prepared according to literature protocols.[2]

2,2',2''-(10-(5-(2-(methoxy)acetamido)-1-carboxypentyl)-1,4,7,10-tetraazacyclododecane-1,4,7-triyl)triacetic acid (9)

2,2',2''-(10-(5-Amino-1-carboxypentyl)-1,4,7,10-tetraazacyclododecane-1,4,7-triyl)triacetic acid (**5**) (0.572 g, 1.20 mmol) and diisopropylethylamine (1.05 mL, 1.26 mmol) were dissolved in dry DMF (10 mL). After 5 min 2,5-dioxopyrrolidin-1-yl 2-methoxyacetate (**6**) (0.269 g, 1.44 mmol) was added and stirring continued for 24 h. The solvent was evaporated and the residue purified by preparative HPLC (Method 1) to yield 0.580 g (1.06 mmol, 88%) of white solid product.

^{1}H (d_6-DMSO, 500 MHz, 60 °C): δ = 7.69 (s, 1H, NH), 7.35 (br.s, 2H, NH), 3.78 (s, 2H, $NHCOCH_2OCH_3$), 3.47 (m, 6H, $3xCH_2CO_2H$), 3.33 (m, 1H, $CHCH_2CH_2CH_2CH_2$) 3.30 (s, 3H, $NHCOCH_2OCH_3$), 3.10-2.77 (m, 18H, cyclen + $CHCH_2CH_2CH_2CH_2$), 1.69-1.55 (m, 2H, $CHCH_2CH_2CH_2CH_2$), 1.44 (pseudo q (J = 6.9 Hz), 2H, $CHCH_2CH_2CH_2CH_2$), 1.33 (m, 2H, $CHCH_2CH_2CH_2CH_2$).

^{13}C (d_6-DMSO, 125 MHz, 60 °C): δ = 172.6, 171.0, 169.9, 168.6, 71.5, 63.6, 58.4, 55.0, 54.8, 51.5, 51.3, 49.3, 47.2, 38.0, 28.8, 27.3, 23.6.

LC/MS (ESI+): $C_{27}H_{48}N_6O_{12}$: m/z calcd 649.34 [MH+]; found 649.6 (MH+)

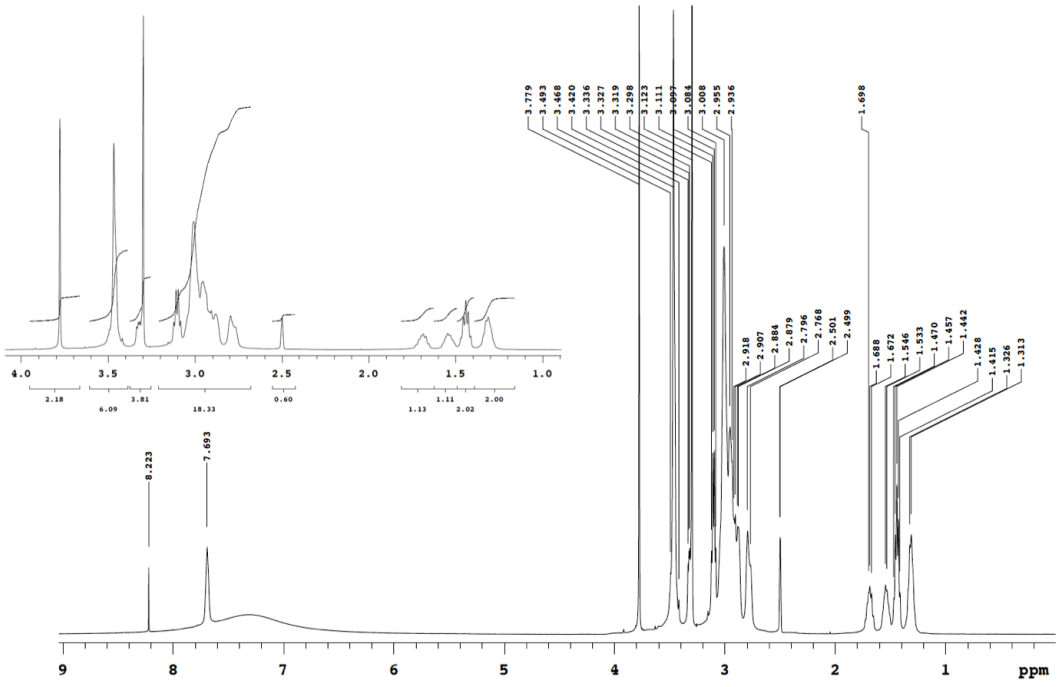

Fig. S23:-^{1}H NMR of (**9**)

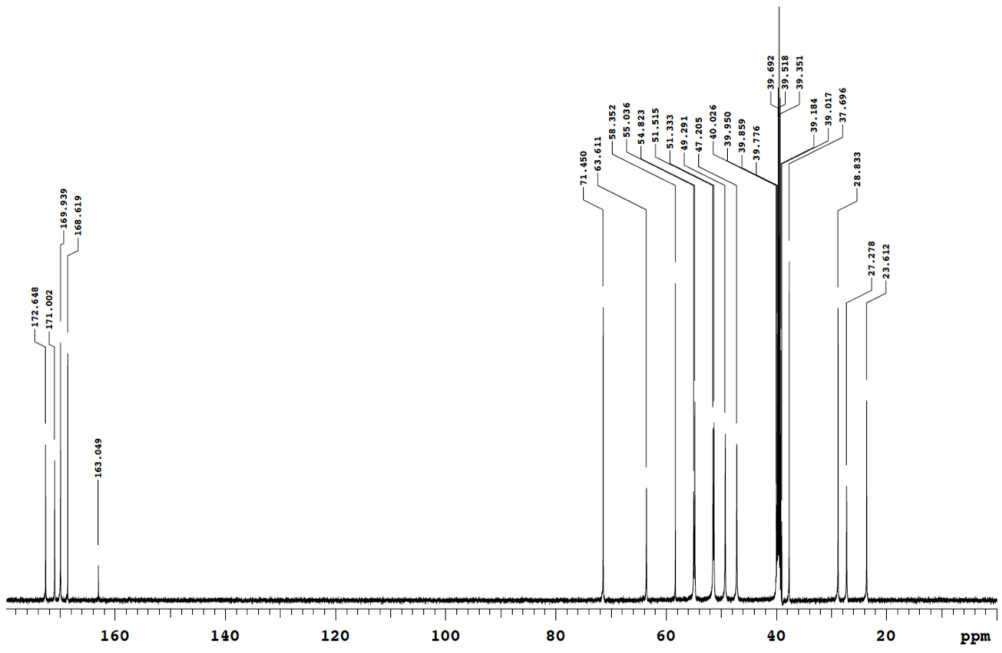

Fig. S24:-^{13}C NMR of (**9**)

2,2',2''-(10-(5-(2-(methoxy)acetamido)-1-carboxypentyl)-1,4,7,10-tetraazacyclododecane-1,4,7-triyl)triacetic acid gadolinium complex (GdOX)

The stock solution of 2,2',2''-(10-(5-(2-(methoxy)acetamido)-1-carboxypentyl)-1,4,7,10-tetraazacyclododecane-1,4,7-triyl)triacetic acid (0.10 g, 0.18 mmol (solid was redissolved in water and subjected to a UV titration using arsenazo III to determine the exact concentration of ligand)) was treated with $GdCl_3.6H_2O$ (0.071 g, 0.19 mmol) and the pH adjusted to 6.2. After 12 h of stirring at r.t., the pH was adjusted to 5.5 and the solution passed through a chelex column. The pH was adjusted to 7.0 and the solution lyophilized to yield a white solid (0.122 g, 0.17 mmol, 95%).

LC/MS (ESI+): $C_{22}H_{36}GdN_6O_{10}$: m/z calcd 703.17 [MH+]; found 703.2 (MH+)

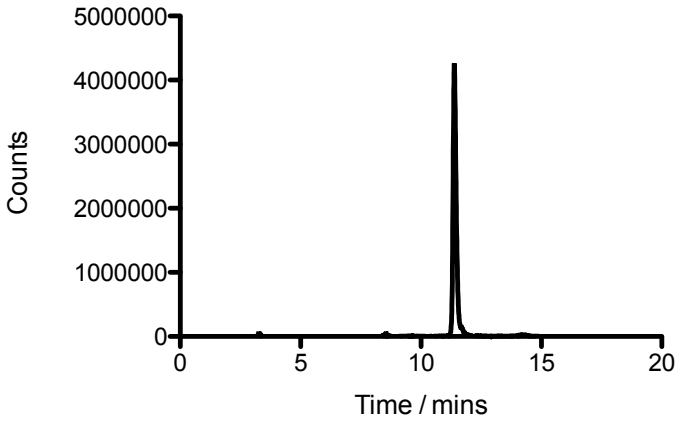

Fig. S25: HPLC-ICP-MS 'Gd' analysis of GdOX

Methods

Relaxivity and BSA binding assay:

Preparation of oxidized BSA, BSA-ALD: Sodium aspartate (13 mg) was added to a solution of bovine serum albumin (BSA) (100 mg) dissolved in phosphate buffered saline (2 mL, pH 7.4, 0.25 mM), followed by the addition of a solution of ferric chloride (10 µL, 10 mM) and left to stir at room temperature overnight. A BSA protein standard without the addition of ferric chloride was run in parallel as a control. Both protein mixtures were purified on PD-10 Sephadex G25 desalting columns (GE Healthcare), eluted with PBS. Protein concentrations were assessed using the 'BCA Protein Assay Kit' (Thermo Scientific). The functionalized protein (BSA-ALD) had a concentration of 20 mg/mL, whilst the control protein (BSA) had a concentration of 18.4 mg/mL. The aldehyde concentration of each protein was estimated using a standard literature DNPH assay protocol. BSA-ALD had an aldehyde concentration of 16 nmol aldehyde/mg of protein, BSA had an aldehyde concentration on 1.2 nmol aldehyde/mg of protein.

Relaxivity measurements: Aliquots of BSA-ALD (3 mg, 150 µL) or BSA (3 mg, 163 µL) were treated for 24 h at 37 ^{o}C with either GdOA or GdOX at a range of concentrations (0.1-1.0 mM), with a total volume of 300 µL maintained for all samples. After 24 h, longitudinal (T_1) relaxation measurements were recorded using a Bruker mq20 Minispec at 1.41 T and 37 ^{o}C. Longitudinal (T_1) relaxation was acquired via an inversion recovery experiment on 10

inversions of duration ranging between 0.05 x T_1 and 10 x T_1. Relaxivity (r_1) was determined from the slope of a plot of $1/T_1$ vs [Gd] for 7 concentrations of Gd(III).

Solutions of GdOA and GdOX (concentration range: 0.1 mM-1.0 mM), in PBS were run in parallel as standard controls.

Protein binding measurements: Gd probe in solution was separated from BSA-bound Gd probe by ultrafiltration (5,000 Da cut-off PLCC cellulosic membrane, 30 mins, 10,000 RPM). Following separation, the concentrated protein residue was diluted to a total volume of 300 µL in PBS and longitudinal (T_1) relaxation measurements of the protein bound and free-solution fractions measured. Quantification of the Gd concentration in each fraction was then determined using an Agilent 8800 ICP-MS system.

Aorta binding studies:
*Elastin preparation***:** Elastin from porcine aorta was purified using the mild method reported by Umeda[3]. Briefly, after removing connective tissue and lipids, aorta was cut into small pieces and suspended in 1 M NaCl for 24 h. The 1M NaCl was replaced and the washing procedure repeated for a further 2 x 24 h. The aorta segments were washed with water and defatted with chloroform:methanol (2:1) for 48 h. The aorta was then lyophilized.

Binding measuremeants
25 mg of lyophilized aorta were treated for 24 h at 37 ^{o}C with either GdOA or GdOX at a range of concentrations (0.1-1.0 mM), with a total volume of 500 µL maintained for all samples. After 24 h aorta segments were washed three x 15 mins in fresh PBS to remove any non-specific bound probes. Aorta segments were then digested in conc. HNO_3 for 24 h at 37 ^{o}C and Gd concentration in each sample was then determined using an Agilent 8800 ICP-MS system.

Transmetallation
Transmetallation stability studies were performed using an adaptation of a literature protocol. [4] To a solution containing a Gd complex (Gd-DTPA or GdOA) was added $Zn(OTf)_2$ solution and phosphate buffer (pH 7.0), affording a solution with 1.0 mM Gd (in total), 1.0 mM Zn, and 67.0 mM phosphate (pH 7.0). The mixture was shaken for 6000 mins at 37 °C. At regular time intervals, the longitudinal relaxation rate ($R_1 = 1/T_1$) of the reaction mixture was measured at 60 MHz. The R_1 value was standardized by measurements made in the absence of Zn^{II}. The remaining ratio (%) of the Gd complexes in the reaction mixture was estimated by eq S1,

$$\%\text{Remaining} = [(R_1 - R_1^{\circ})/(R_1^{\text{init}} - R_1^{\circ})] \times 100\% \qquad \text{(S1)}$$

where

R_1°: R_1 for buffer solution (which did not contain the Gd complexes), 0.5 s^{-1}.
R_1^{init}: R_1 at t = 0 hr in the presence of Gd complexes. 8.2 s^{-1} for Gd-DTPA and 8.6 s^{-1} for Gd-OA.

The arbitrarily defined kinetic index is given as the time required for $R_1(t)$ to reach 80% of the initial $R_1(0)$ value.

Animal protocol

All experiments and procedures were performed in accordance with the National Institutes of Health's "Guide for the Care and Use of Laboratory Animals" and were approved by the Massachusetts General Hospital Institutional Animal Care and Use Committee.

Lung fibrosis model: C57Bl/6 adult male mice at 6 weeks of age (Charles River Laboratories, Wilmington MA) received a single dose of bleomycin (Fresenius Kabi, Lake Zurich, Il), prepared in sterile PBS. Bleomycin was intratracheal injected at 1.0 units/kg body weight (50 µL total volume). Images with GdOA or the control GdOX were carried out after 2 weeks (advance disease state).

To evaluate Gd-OA sensitivity to detecting treatment response, β-aminopropionitrile (BAPN), a pan-LOX inhibitor, was prepared in PBS, and dosed at 100 mg/kg. Starting on the day of bleomycin instillation, each mouse was dosed daily with BAPN via IP injection. Controls similarly underwent bleomycin instillation, and injected daily with PBS. GdOA MRI was performed after 2 weeks.

A total of 46 C57Bl6 mice were included to study pulmonary fibrosis:

A. Intratracheal bleomycin instillation, imaged after 2 weeks (n=22), 18 were imaged with Gd-OA and 4 were imaged with Gd-OX.
B. Intratracheal PBS instillation as Sham control (n=16), 12 were imaged with Gd-OA, 4 were imaged with Gd-OX.
C. Intratracheal bleomycin instillation, with daily I.P. BAPN, n=5 were imaged at 2 week with Gd-OA.
D. Intratracheal bleomycin instillation, with daily I.P. PBS as control n=3 were imaged at 2 week with Gd-OA.

All animals were sacrificed after imaging for biochemical analysis and histological analysis.

MR imaging

At the time of imaging, pre-injection baseline images as well as post-injection images were acquired for comparison. Probes (GdOA or GdOX) were administrated via intravenous bolus injection at 100 nmol Gd/ g body weight, with the bolus volume of injection never exceeding 100 µL. Concentration of GdOA and GdOX was determined by ICP-MS.

Mice were imaged on a 9.4 Tesla MRI scanner (Bruker, Billerica MA) using a custom-built volume coil. Animals were anesthetized with 1–2% isoflurane and air/oxygen mixture to maintain constant respiration rate, kept warm by a thermal pad, and monitored by a small animal physiological monitoring system (SA Instruments Inc., Stony Brook NY).

Lung fibrosis imaging protocol: Images were acquired with the following sequences and parameters: 3D Ultra Short TE (UTE) sequence with respiratory gating (Matrix 192 x 192; TR/TE/flip angle = 8ms/0.02ms/40°; field of view (FOV) 48 x 48 mm; one average; slice thickness=250µm, acquisition time=30 minutes, spatial resolution=250µm isotropic); 3D Fast Low Angle Shot (FLASH) (Matrix 96 x 192; TR/TE/FA=15 ms/1.5 ms/40°; field of view (FOV) 24 x 48 mm; one average; slice thickness=250 µm, acquisition time=2-3 minutes, spatial resolution=250 µm isotropic); T1-weighted Rapid Acquisition with Relaxation Enhancement (RARE) (Matrix 192 x 192; TR/TE/FA=1000 ms/26 ms/180°; field of view (FOV) 33 x 33 mm; one average; slice thickness=1mm, acquisition time=2 minutes, spatial

resolution=172 μm). After a localizer image to position the animal, RARE images were acquired in coronal and axial orientations to provide images with good anatomical contrast. This was followed by baseline FLASH and UTE images. The probe was delivered as a bolus via an indwelling tail vein catheter. Immediately after injection the FLASH sequence was repeated 5 times to demonstrate probe injection and to measure clearance of probe from the blood and other organs. At 12 min post-injection, the UTE image was repeated.

Lung image representation: A subtraction image was generated in Osirix (Geneva, Switzerland) by subtracting the UTE pre probe injection image from the UTE post probe injection image. A mask was applied to the lung based on the anatomical scan. The resulting difference image was then false colored, and superimposed on the corresponding anatomical scan image.

Lung image analysis: We first visualized the vasculature on the anatomical coronal images (T1-weighted RARE sequence) to delineate lung parenchyma from vessels and airways to define the regions of interest (ROI). The FLASH image immediately post injection was also used to identify large vessels. One ROI, excluding large vessels and airways, was placed over the left lung and one ROI was placed over the right lobes of the lung; additional ROIs were placed over the left forearm muscle and the right forearm muscle. These ROIs were then copied onto the UTE images to quantify signal intensity (SI). Coronal slices that cover the entire lung were analyzed (>10 250 μm slices per mouse). The lung ROI size ranged from 0.5-41.4 mm^2 with 10-20 ROIs used to cover the entire lung. The analysis was repeated for the pre-probe and post-probe UTE data sets. Image visualization and quantification was performed in Osirix.

To quantify signal enhancement in the lung, lung to muscle ratio (ΔLMR) was calculated according to equation S2 where SI=signal intensity average of all image slices was calculated for the pre-injection images (LMR_{pre}) and for the post-injection images (LMR_{pos}). The lung enhancement for each mouse is expressed as ΔLMR, the difference between the pre-injection LMR and the post-injection LMR (equation S3.

$$LMR = SI_{lung} / SI_{muscle} \quad (S2)$$

$$\Delta LMR = LMR_{post} - LMR_{pre} \quad (S3)$$

Hydroxyproline assay

In a high-pressure reaction tube containing 250 μL lung homogenate was added 150 μL water, 100 μL 4 mM sarcosine as an internal standard, and 500 μL 12 M HCl. The reaction vessel was capped with a teflon cap and heated at 110 °C for 24 h. After hydrolysis the reaction solution was cooled to r.t. and neutralized with 6M NaOH. To 100 μL of the supernatant was added 900 μL borate buffer (0.7 M boric acid, pH 9.5) in a glass tube. Next 100 μL of *o*-phthaladehyde (50 mg) dissolved in 1 mL acetonitrile containing 26 μL of β-mercaptoethanol was added, followed 60 s later by 100 μL of iodoacetamide reagent (140 mg/mL of iodoacetamide in acetonitrile). One minute later, 300 μL of 5mM FMOC in acetone was added with vortexing. Five minutes after FMOC addition, 3 mL of ethyl ether was added and the reaction vortexed. The organic layer was discarded and the wash repeated. The aqueous phase was then diluted with 5 mL water. Hydroxyproline standards were prepared with hydroxyproline:sarcosine ratios of 1:4, 1:2, 1:1, 2.5:1 and 5:1 at a constant concentration of sarcosine of 100 μM. Standards and tissue samples were then subject to

HPLC analysis. The hydroxyproline:sarcosine peak ratio was used to quantify hydroxyproline concentration.

Allysine assay

The allysine concentration in murine lung tissue samples was quantified using an adaption of the p-cresol protocol of [5]. *p*-Cresol was replaced with fluorescent sodium 2-naphthol-7-sulfonate to increase the sensitivity of detection. In a high-pressure reaction tube containing 250 µL lung homogenate was added 200 µL water, 50 µL 4 mM fluorescein as an internal standard, 500 µL 12 M HCl and 20 mg of sodium 2-naphthol-6-sulfonate (TCI America). The reaction vessel was capped with a teflon cap and heated at 110 ^{o}C for 24h. The reaction solution was cooled, neutralized with 6 M NaOH and analysed by HPLC.

HPLC conditions: Solvent A: H_2O + 0.1% TFA, Solvent B: MeCN + 0.1% TFA. 0-40 mins; 5-30% solvent B, 40-42 mins; 30-95% solvent B, 42-45 mins; 95% solvent B, 45-47 mins; 95-5% solvent B, 47-50 mins; 5% solvent B. Column: C8 Phenomenex 25 mm x 4 mm, 5 µm. 0-40 mins λ_{ex} = 254, λ_{em} = 310 nm, 40-50 mins λ_{ex} = 490 nm, λ_{em} = 510 nm.

Peak areas were corrected according to a fluorescein standard (elution time: 45 mins) and allysine concentration in nmol/Lung calculated using a standard curve (plot of concentration of the pure bis-naphthol derivative of allysine vs. HPLC peak area), and a correction for lung mass.

LOX assay protocol

Enzymatic activity measurement was based on the production of H_2O_2 [6] [7].

LOX extraction:

Protease inhibitors (PI) (2X, PBS buffer) (0.25 mL) were added to 0.25 mL of freshly prepared lung homogenate, and left for 4 h at 4 °C on a bench shaker. Lung homogenate was then spun down (13,000 rpm, 20 mins, 4 °C), supernatant removed, and the pellet washed twice with PBS buffer. The remaining pellet was re-suspended in 4 M Urea, 50 mM sodium borate buffer, pH 8.2 buffer, and left overnight at 4 °C on a bench shaker. Lung homogenate was spun down (13,000 rpm, 20 mins, 4 °C), the supernatant underwent buffer exchange and concentrated at 4 °C using a 10k MWCO centrifugal filter (Millipore) to give a final volume of 300 µL in 1.2 M urea, 50 mM sodium borate buffer, pH 8.2.

Fluorescence assay:

Lung samples were incubated with 0.5 mM of pargyline, to inhibit any potential endogenous monoamine oxidase A and B. In a 96 well plate (Greiner 96 Well Black Microclear Base), 100 µL of tissue homogenate was incubated with 20 µL of pargyline for 1 h at 37 °C with or without the pan-LOX inhibitor, BAPN (100 µM). A reaction mixture containing Amplex Red (125 µM- for a final concentration 50 µM), horseradish peroxidase (2.5 U/ml- for a final concentration 1 U/ml) and diaminopentane (37.5 µM – for a final concentration 15 µM) was prepared in 1.2 M urea, 50 mM sodium borate buffer, pH 8.2. 80 µL of the reaction mixture was added into each well after the 1 h incubation. The relative fluorescence units (RFU) were read every 1 min for 60 min at 37 °C, excitation 565 nm and emission 590 nm, and the slope of the kinetic curves for each sample in the linear range was calculated using PRISM data analysis software. The difference between the signals obtained in the presence of the BAPN inhibitor and in the absence of the inhibitor was considered to be the specific total LOX activity in the sample.

Slopes of the data in RFU/min were converted to pmol H_2O_2/min/Lung using a standard curve of [H_2O_2] vs. RFU and a correction for lung mass.

Statistics

Unless otherwise noted, the results are expressed as means ± 1 standard deviation. Statistical analyses were performed using GraphPad Prism 5 software (LA Jolla, CA). The comparisons between a treatment group and Naive group were analyzed by an unpaired t-test. A one-way ANOVA, followed by post hoc Tukey tests with two-tailed distribution was used for analyzing the data between different groups. A p value of less than 0.05 was considered significant.

References

[1] aD. A. Moore*, Vol. WO2007106546 A2*, **2012**;bS. Foillard, M. O. Rasmussen, J. Razkin, D. Boturyn, P. Dumy, *J. Org. Chem.* **2008**, *73*, 983-991.

[2] R. B. Greenwald, A. Pendri, D. Bolikal, *J. Org. Chem.* **1995**, *60*, 331-336.

[3] H. Umeda, K. Kawamorita, K. Suyama, *Amino acids* **2001**, *20*, 187-199.

[4] S. Laurent, L. V. Elst, F. Copoix, R. N. Muller, *Investigative radiology* **2001**, *36*, 115-122.

[5] H. Umeda, K. Kawamorita, K. Suyama, *Amino acids* **2001**, *20*, 187-199.

[6] R. B. Rucker, N. Romero-Chapman, T. Wong, J. Lee, F. M. Steinberg, C. McGee, M. S. Clegg, K. Reiser, T. Kosonen, J. Y. Uriu-Hare, J. Murphy, C. L. Keen, *The Journal of nutrition* **1996**, *126*, 51-60.

[7] H. C. Schilter, A. Collison, R. C. Russo, J. S. Foot, T. T. Yow, A. T. Vieira, L. D. Tavares, J. Mattes, M. M. Teixeira, W. Jarolimek, *Respiratory research* **2015**, *16*, 42.